

## SUPPLEMENTARY MATERIAL

### Is MIP-OES a suitable alternative to ICP-OES for trace element analysis?

Beatriz M. Fontoura<sup>a</sup>, Florencia Cora Jofré<sup>b,c</sup>, Trey Williams<sup>d</sup>,  
Marianela Savio<sup>b,c</sup>, George L. Donati<sup>e\*</sup> and Joaquim A. Nóbrega<sup>a</sup>

<sup>a</sup>Group for Applied Instrumental Analysis, Department of Chemistry, Federal University of São Carlos, P.O. Box 676, São Carlos, SP, 13565-905, Brazil.

<sup>b</sup>Facultad Ciencias Exactas y Naturales, Universidad Nacional de La Pampa, Santa Rosa, La Pampa, Argentina.

<sup>c</sup>Consejo Nacional de Investigaciones Científicas y Técnicas de Argentina (CONICET), Instituto de Ciencias de la Tierra y Ambientales de La Pampa (INCITAP), Santa Rosa, La Pampa, Argentina.

<sup>d</sup>Department of Chemistry, Clemson University, Clemson, SC 29634, USA.

<sup>e</sup>Department of Chemistry, Wake Forest University, Salem Hall, Box 7486, Winston Salem, NC 27109, USA.

\*Corresponding author: George L. Donati  
E-mail: donatigl@wfu.edu

## Abbreviations

AAS	Atomic absorption spectrometry
AD	Aerosol dilution
BG	Spectral background
CCD	Charge-coupled device detector
CN	Conventional nebulization
CRM	Certified reference material
$C_{\text{sam}}$	Concentration of analyte in the sample
CV	Cold vapor generation
DLLME	Dispersive liquid-liquid microextraction
DSPE	Dispersive solid-phase extraction
EC	External standard calibration
EF	Enrichment factor
EGCM	External gas control module
EIEs	Easily ionized elements
$E_{\text{sum}}$	Total energy
FAAS	Flame atomic absorption spectrometry
FI	Flow injection
GLS	Gas-liquid separation
HG	Hydride generation
ICP-OES	Inductively coupled plasma optical emission spectroscopy
IS	Internal standardization
LDR	Linear dynamic range
LOD	Limit of detection
LOQ	Limit of quantification
LTE	Local thermal equilibrium
MEC	Multi-energy calibration
MF	Magnetic field
MFC	Multi-flow calibration
MICAP	Microwave-sustained inductively coupled atmospheric-pressure plasma
MIP-OES	Microwave-induced plasma optical emission spectrometry
MMC	Matrix-matching calibration
MP-AES	Microwave plasma atomic emission spectrometry
MS	Mass spectrometry
MSIS	Multimode sample introduction system
MSPE	Magnetic solid-phase extraction
MW	Microwave radiation
$n_e$	Electron number density
NGFR	Nebulization gas flow rate
OES	Optical emission spectrometry
PVG	Photochemical vapor generation
REEs	Rare-earth elements
RF	Radiofrequency
RSD	Relative standard deviation
SA	Standard additions
S/B	Signal-to-background-ratio
SDA	Standard dilution analysis

SPE	Solid phase extraction
SPME	Solid phase microextraction
S1	First solution (sample and standard)
S2	Second solution (sample and blank)
TD	Thermal desorption
TDS	Total dissolved solids
$T_e$	Electron temperature
$T_g$	Gas temperature
Vis	Visible region of the electromagnetic spectrum
VP	Viewing position
$W_{tot}$	Analyte mass transported to plasma

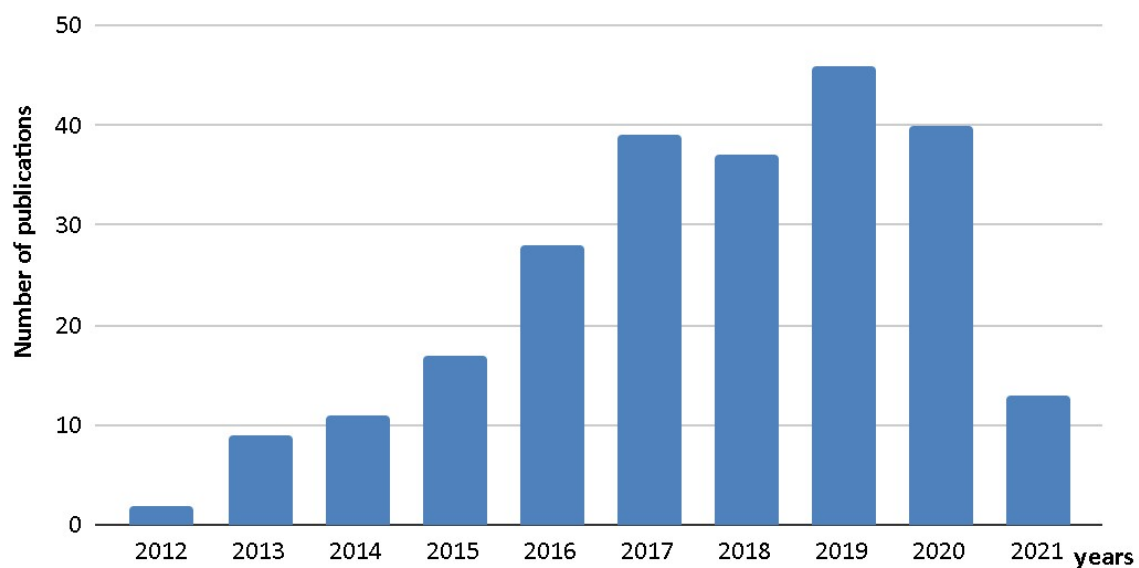


**Figure S1.** MIP-OES publications since the Agilent MP-AES release in 2012, according to the Web of Science.

**Table S1.** Limits of detection ( $\mu\text{g L}^{-1}$ ) calculated for different elements in several samples analyzed by MIP-OES and ICP-OES.

Sample	Analyte	MIP-OES		ICP-OES		Ref.
		Emission line (nm)	LOD ( $\mu\text{g L}^{-1}$ )	Emission line (nm)	LOD ( $\mu\text{g L}^{-1}$ )	
Fertilizer and animal feed	Cu	324.754 - I	2.2	324.754 - I (N)	1.7	1
	Fe	259.940 - II	4.1	259.940 - II (N)	1.8	
	Mn	257.610 - II	1.5	257.610 - II (N)	5.4	
	Zn	213.857 - I	2.3	213.857 - I (N)	1.8	
Bio sludge	B	249.677 - I	1.0	249.677 - I (A)	1.0	2
	P	213.618 - I	25	213.618 - I (A)	30	
	Mo	379.825 - I	2.0	379.825 - I (A)	3.0	
Sewage sludge, fired brick, and sediment	Cd	228.802 - I	32.9	228.802 - I (N)	4.6	3
	Cr	267.716 - II	38.8	425.433 - I (N)	63.4	
	Cu	324.754 - I	32.7	324.754 - I (N)	28.2	
	Ni	216.555 - II	33.5	352.454 - I (N)	52.3	
	Pb	220.353 - II	28.8	405.781 - I (N)	345	
	Zn	213.857 - I	26.0	213.857 - I (N)	70.9	
Instant soup <sup>a</sup>	Ca	-	-	422.673 - I (R)	0.318	4,5
	Cu	324.754 - I	0.090	324.754 - I (R)	0.316	
	K	769.897 - I	4.9	769.896 - I (R)	12.2	
	Mg	285.213 - I	1.0	285.213 - I (R)	0.129	
	Mn	403.076 - I	0.040	257.610 - II (R)	0.173	
	Na	-	-	588.995 - I (R)	1.50	
	P	213.618 - I	5.4	178.284 - I (R)	1.05	
	Zn	213.857 - I	0.88	213.856 - I (R)	0.214	

Water for injections <i>(Aqua ad injectabilia)</i>	Al	394.401 - I	0.8	394.401 - I (A)	0.6	6
and high-purity water <i>(Aqua valde purificata)</i>	Al	396.152 - I	0.7	396.152 - I (A)	0.4	
Crude oil <sup>a</sup>	Ca	396.847 - II	NR	317.930 - II (R)	0.01	7
	Fe	259.940 - II	0.01	238.204 - II (R)	0.01	
	K	769.897 - I	0.06	769.897 - I (R)	0.01	
	Na	588.995 - I	0.07	588.995 - I (R)	0.02	
	Ni	341.476 - I	NR	221.650 - II (R)	0.01	
	V	311.070 -II	NR	292.460 - II (R)	0.01	
Vinegar	Al	396.152 - I	0.62	NA	NA	8
	B	249.772 - I	7.67	NA	NA	
	Co	340.512 - I	4.55	NA	NA	
	Cr	425.433 - I	0.52	NA	NA	
	Mn	403.076 - I	0.35	NA	NA	
	Pb	405.781- I	2.42	NA	NA	
Leather and fur <sup>a,b</sup>	Cd	228.802 - I	1.3	228.802 - I (A)	0.6	9
	Co	350.228 - I	1.9	238.892 - II (A)	1.0	
	Cr	427.480 - I	0.9	205.560 - II (A)	0.9	
	Cu	327.395 - I	1.5	327.395 - I (A)	1.0	
	Hg	253.652 - I	2.0	194.164 -II (A)	2.0	
	Ni	341.476 - I	0.9	231.604 - II (A)	1.4	
	Pb	405.781 - I	1.2	220.353 - II (A)	5.0	
Agricultural samples <sup>b</sup>	As	188.979 - I	0.46	NA	NA	

	Bi	223.061- I	0.094	NA	NA	10
	Ge	265.117- I	0.19	NA	NA	
	Sb	217.581 - I	0.46	NA	NA	
	Sn	303.412 - I	5.2	NA	NA	
Diesel and biodiesel	Si	251.611 - I (nitric acid)	20	NA	NA	
	Si	251.611 - I (Microemulsion)	5	NA	NA	11
	Si	288.158 - I (nitric acid)	240	NA	NA	
	Si	288.158 - I (Microemulsion)	5	NA	NA	
Ethanol fuel	Cr	425.433 - I	0.7	NA	NA	
	Ni	352.454 - I	20	NA	NA	12
	Pb	405.781 - I	40	NA	NA	
	V	437.923 - I	0.3	NA	NA	
Fish <sup>a</sup>	As	234.984 - I	0.02	NA	NA	
	Cd	228.802 - I	0.01	NA	NA	
	Cu	324.754 - I	0.12	NA	NA	13
	Pb	405.781 - I	0.07	NA	NA	
	Hg <sup>†</sup>	253.652 - I	0.01	NA	NA	

<sup>a</sup> LODs values expressed mg kg<sup>-1</sup>.

<sup>b</sup> Obtained with a multimode sample introduction system by MIP-OES (HG-MIP-OES).

I- atomic line, II- ionic line; N, A and R represent plasma viewing not informed, axial and radial, respectively.

NA- Not determined.

NR - Not reported. The LOD reported by the authors was 0.00 µg L<sup>-1</sup>. We prefer the term not reported in this case.

**Table S2.** MP-AES commercially available models and their general characteristics.<sup>a</sup>

<b>Agilent MP-AES</b>	<b>4100</b>	<b>4200</b>	<b>4210</b>	<b>Improvement</b>
<b>Waveguide</b>	Microwave assembly (waveguide), Part number: G8000-64126	Improved waveguide	Improved waveguide	Increases the torch useful life and long-term stability
<b>Number of temperature sensors</b>	1	2	2	Better waveguide and magnetron temperature control
<b>Torch design</b>	Easy-fit, black base	Easy-fit, blue base with a thicker wall <sup>b</sup>	Easy-fit, blue base with a thicker wall <sup>b</sup>	Contributes to higher plasma temperature and improves performance with difficult samples (high TDS), reducing cleaning time and downtime
<b>Total dissolved solids (TDS)</b>	1 % maximum	3 % maximum	3 % maximum	More robust torch assembly, without compromising LODs

<sup>a</sup> Pat. N°s: US006683272B2, US007030979B2, US009345121B2, US009247629B2

<sup>b</sup> Not compatible with earlier model 4100 MP-AES

**Table S3.** Performance of nebulizers used with MIP-OES.<sup>14</sup>

Nebulizer	Parameter		Performance depending on the matrix					
	Plasma excitation temperature	Plasma $n_e$	Solvent transport efficiency	LOD	HNO <sub>3</sub> (1 % v/v)	H <sub>2</sub> SO <sub>4</sub> (1 % v/v)	EIEs (100 mg L <sup>-1</sup> Na, K and Ba)	Ethanol (1 % v/v)
OneNeb® series 1								
OneNeb® series 2	Lowest	Lowest	Highest	Lowest	Best	Best		Best
Mira Mist®	Highest	Highest	Lowest			Best		
Concentric				Highest	Worst	Worst	Worst	Worst

## References

- 1 W. Li, P. Simmons, D. Shrader, T. J. Herrman and S. Y. Dai, *Talanta*, 2013, **112**, 43–48.
- 2 V. Sreenivasulu, N. S. Kumar, V. Dharmendra, M. Asif, V. Balaram, H. Zhengxu and Z. Zhen, *Appl. Sci.*, 2017, **7**, 1–10.
- 3 F. Baraud, A. Zaiter, S. Porée and L. Leleyter, *SN Appl. Sci.*, 2020, **2**, 1536.
- 4 L. São Bernardo Carvalho, C. Santos Silva, J. Araújo Nóbrega, E. Santos Boa Morte, D. C. Muniz Batista Santos and M. G. Andrade Korn, *J. Food Compos. Anal.*, 2020, **86**, 103376.
- 5 A. Krejčová, T. Černohorský and D. Meixner, *Food Chem.*, 2007, **105**, 242–247.
- 6 T. O. Samarina, D. S. Volkov, I. V. Mikheev and M. A. Proskurnin, *Anal. Lett.*, 2018, **51**, 659–672.
- 7 J. Nelson, G. Gilleland, L. Poirier, D. Leong, P. Hajdu and F. Lopez-Linares, *Energy and Fuels*, 2015, **29**, 5587–5594.
- 8 N. Ozbek, M. Koca and S. Akman, *Food Anal. Methods*, 2016, **9**, 2246–2250.
- 9 Y. Zhao, Z. Li, A. Ross, Z. Huang, W. Chang, K. Ou-Yang, Y. Chen and C. Wu, *Spectrochim. Acta - Part B At. Spectrosc.*, 2015, **112**, 6–9.
- 10 R. C. Machado, C. D. B. Amaral, J. A. Nóbrega and A. R. A. Nogueira, *J. Agric. Food Chem.*, 2017, **65**, 4839–4842.
- 11 R. S. Amais, G. L. Donati, D. Schiavo and J. A. Nóbrega, *Microchem. J.*, 2013, **106**, 318–322.
- 12 G. L. Donati, R. S. Amais, D. Schiavo and J. A. Nóbrega, *J. Anal. At. Spectrom.*, 2013, **28**, 755–759.
- 13 S. E. Gallego Ríos, G. A. Peñuela and C. M. Ramírez Botero, *Food Anal. Methods*, 2017, **10**, 3407–3414.
- 14 A. B. S. Silva, J. M. Higuera, C. E. M. Braz, R. C. Machado and A. R. A. Nogueira, *Spectrochim. Acta - Part B At. Spectrosc.*, 2020, **168**, 105867.